RSC Advances

This article can be cited before page numbers have been issued, to do this please use: G. Angajala and R. Subashini, *RSC Adv.*, 2015, DOI: 10.1039/C5RA06593C.

ROYAL SOCIETY OF CHEMISTRY

www.rsc.org/advances

View Article Online
DOI: 10.1039/C5RA06593C

Nickel nanoparticles: A highly efficient and retrievable catalyst for the solventless friedlander annulation of quinolines and their *in-silico* molecular docking studies as histone deacetylase inhibitors.

Gangadhara Angajala, R. Subashini*

Chemistry Research Laboratory, Organic Chemistry Division. School of Advanced Sciences, VIT University, Vellore - 632014.

*Corresponding author:
Tel.: +91 94435 41305, +91 0416 2202352.
Email address: dr.subashini.r@gmail.com (Dr. R. Subashini)

Graphical Abstract

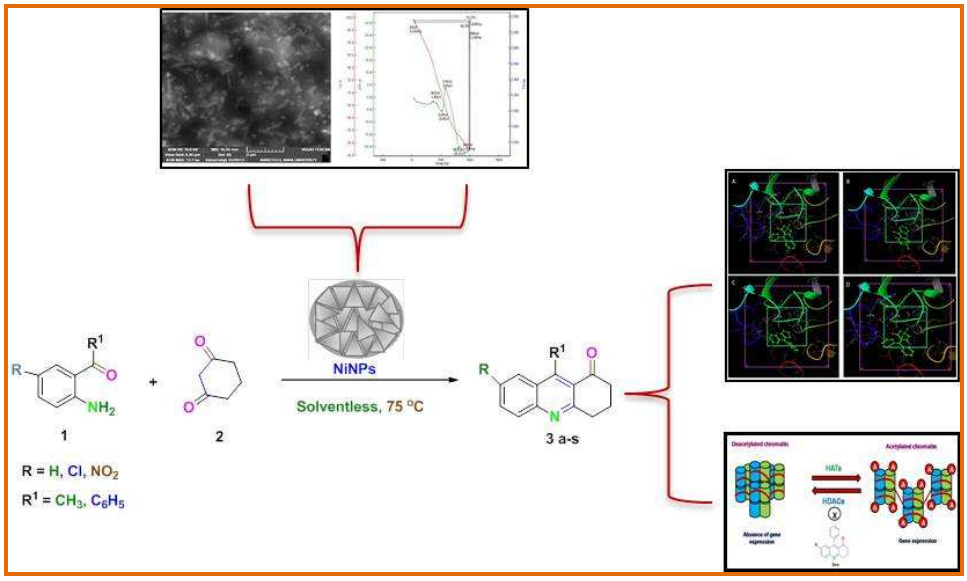

Dynamic Article Links ► View Article Online DOI: 10.1039/C5RA06593C

Cite this: DOI: 10.1039/c0xx00000x

www.rsc.org/xxxxxx

ARTICLE TYPE

Nickel nanoparticles: A highly efficient and retrievable catalyst for the solventless Friedlander annulation of quinolines and their *in-silico* molecular docking studies as histone deacetylase inhibitors

Gangadhara Angajala, R. Subashini*

Received (in XXX, XXX) Xth XXXXXXXXX 20XX, Accepted Xth XXXXXXXXX 20XX
DOI: 10.1039/b000000x

The present work explores a highly efficient, environmental friendly, green, solvent-free protocol for the preparation of polysubstituted quinolines *via* Friedlander annulation using nickel nanoparticles (80-100 nm) biofabricated from *Aegle Marmelos* Correa aqueous leaf extract. These nickel nano materials exhibit high catalytic efficacy to achieve the target molecules in excellent yields ranging from 85-96 % mainly due to their diverse properties and high surface area to volume ratio. The synthesized polysubstituted quinolines were successfully characterized by FT-IR, ^{1}H NMR, ^{13}C NMR, and GC-MS. The effect of various solvents and catalyst concentration on the synthesis of quinolines has been investigated where under solventless conditions at10 mol % of the nickel nano catalyst high yields of the product were obtained. Reusability of the catalyst up to five cycles under solvent-free conditions within shorter reaction time, without any significant loss in the yields of the product are the unique features of this heterogenous solid catalysis. Furthermore safer reaction profiles, high selectivity, greater yields, reliable cost efficiency, simple workup conditions are some of the noteworthy highlights of this green ecofriendly process. *In-silico* molecular docking studies for anticancer efficacy of the quinoline derivatives as histone deacetylase inhibitors (HDIs) were carried out. The results showed that compounds **3h** (-7.3), **3n** (-7.1), **3l** (-6.5) and **3b** (-6.7), are having better binding affinity showing docking score which is greater than that of standard Vorinostat (-6.4) and comparable to that of standard Panobinostat (-7.9).

1 Introduction

Quinolines and their derivatives are considered as important scaffolds in medicinal chemistry because of their wide spectrum of biological activities[1-4]. Annually nearly 2000 tons of quinoline are produced from all over the world indicating its biological importance[5-7]. It is an important heterocyclic intermediate with wide range of applications especially in metallurgical process, polymer industry, agro chemical production and in dye industry[8]. Quinoline moiety also has significant role in the formation of conjugated molecules and polymers that combine enhanced nonlinear optical, optoelectronic properties with excellent pharmacological activities[9-14]. Synthesis of quinoline derivatives and its analogues has been an attractive goal for the synthetic organic chemists due to their pharmacological role as substructures in the wide variety of designer and natural products [15-19]. Quinoline scaffold is present in many medicinal plant alkaloids and with the advancements in the phytochemistry isolation of quinine prompted the development of wide variety of synthetic antimalarials[20-23]. In medicinal chemistry quinolines have wide variety of biological applications such as anti-inflammatory[24], antibacterial[25], antimalarial[26], antifungal[27], antiprotozoal[28], analgesic[29], antiviral[30], antineoplastic[31] and cardiovascular activity[32]. Development of polysubstituted quinolines can achieve hierchical self-assembly into meso and nano structures with enhanced electronics and photonic properties.

In the recent years significant efforts continued to be directed in the development of new quinoline-based structures[33-35] and different newer methods for their construction[36,37]. Over the past decades various chemical methods such as Doebner-von Miller, Skraup, Friedlander and Combes reactions have been developed for the synthesis of quinolines[38-41]. Among the various preparation methods of quinolines reported so far in literature, Friedlander annulation of quinolines is one of the most straight forward and simplest method for the synthesis of quinoline derivatives. It usually starts with the reaction of 2-amino aryl ketones and a second carbonyl compound possessing a reactive α-methylene group which is catalysed by both acids and bases. Bronsted acids such as hydrochloric acid, sulfamic acid, sulphuric acid, p-toluene sulfonic acid and polyphosphoric acid were widely employed as catalysts in the synthesis of quinolines[42]. However most of these methods require very harsh conditions and lead to several side unwanted reactions. In the presence of base catalysts at high temperature, 2-aminobenzophenone fails to react with simple ketones such as cyclohexanone and β-keto esters[43].

Further extensive work on quinoline derivatives showed that acid catalysts are more effective than base catalysts for the Friedlander annulation of quinoline. Lewis acids such as $SnCl_2$, $ZnCl_2$, $Mg(ClO_4)_2$, Sodium fluoride, $FeCl_3$, silverphosphotungstate and $NaAuCl_4.2H_2O$ have been proved to be effective for the synthesis of quinolines[44-48]. Most of the reported methods for the synthesis of quinolines suffer from the usage of harmful organic solvents, high reaction temperature, prolonged reaction times with low yields, tedious work up procedures and use of relative expensive reagents. Therefore in order to avoid limitations associated with normal chemical synthesis there is an effective need to develop easy practical approaches to a variety of quinoline derivatives

View Article Online
DOI: 10.1039/C5RA06593C

with useful pharmacophores. Different researches from all over the world have made use of new catalysts in several well established new methodologies. Besides an array of new and innovative strategies have been developed which has rendered the synthesis of quinoline core a much simpler process than earlier.

Now a day there is huge demand in assembling quinoline systems by nano catalysts for selective, cheap, ecofriendly, low cost protocols for their synthesis[49]. In literature various metal oxide nanoparticles have been used for the Friedlander annulation of quinolines[50,51]. Nano catalysis is currently the subject of considerable attention for synthetic chemists to develop some ecofriendly, environmentally benign techniques because these heterogenous organic reactions have several advantages such as safe handling, ease of disposal, minimum execution time and waste minimization[52,53]. The use of metal nanoparticles in catalysis is crucial as they mimic metal surface activation and catalysis at the nanoscale and thereby bring selectivity and efficiency to heterogeneous catalysis. Metal nanoparticles have tremendous catalytic applications in organic synthesis mainly due to their small size and large surface area[54-57]. Recently nickel nanoparticles are widely employed as catalysts which offer great opportunities for wide range of organic reactions and chemical manufacturing processes including reduction of aldehydes[58] and ketones[59], chemoselective oxidative coupling of thiols[60], hydrogenation of citral[61], styrene oxide[62], synthesis of thioesters[63] and quinoxalines[64].

From the past 100 years Friedlander annulation is a well-known method for the synthesis of quinolines. To handle this particular condensation in smooth manner, we have developed an inexpensive, safe, non-volatile, green nickel nano catalyst biofabricated from *Aegle Marmelos* Correa aqueous leaf extract under optimum reaction conditions nearly 96 % of yields have been achieved. The increasing yields are due to large surface area, surface activity of the catalyst with the effect of reduced time to get the corresponding products in high yield. The purpose of present study was to investigate the feasibility of nickel nano catalyst in the Friedlander annulation of quinolines as an ecofriendly, inexpensive, effective and smooth reaction conditions.

2 Results and discussion

2.1 Chemistry

Catalytic applications of various metal nanoparticles are always advantageous in various organic transformations. The reason for this high efficient catalytic ability was mainly due to its surface area to volume ratio. High surface area to volume ratios have interesting applications such as increased therapeutic and catalytic applications[65]. Nickel nanoparticles are special and interesting mainly because, their physical and chemical properties are totally different when compared to their macro counter parts. Due to their small size nickel nanoparticles possess unique properties, regardless of their chemical properties they generally have high surface area to volume ratio. This automatically causes their physical properties to be dominated by the effect of capping agents and surface atoms on the surface of nickel nanoparticles. The broad band centered at~ 3400 cm^{-1} in the FT-IR spectral analysis of the nickel nanoparticles (80-100 nm) indicates the presence of hydroxyl functional group (Fig.2). The high surface area-to-volume ratio of nickel nanocrystals can sometimes lead to unexpected properties. Particles with high surface area possess many reaction sites than a particle with low surface area and thus lead to higher chemical reactivity. Moreover, as the surface area increases the dominance behaviour of the atoms increases on its outer surface rather than the interior of the particle. Collectively the surface functional hydroxyl groups, highly active Lewis acid sites and other effects play a major role in the Friedlander hetero-annulation of quinolines (Fig.1).

Hence keeping all these facts of nickel, it is considered worthwhile to explore the catalytic applications of biofabricated NiNPs in Friedlander annulation of quinolines. Initially, the reaction was monitored under different solvents and without solvent. The most important property of solvent molecules is the response to the changes associated with charges and their corresponding distribution during the process of a reaction. In order to accommodate the distribution of charges dielectric constant of the solvent is considered as a good indicator. It reduces the field strength of the electric field surrounding the charged particle immersed in the solvent. In general, protic solvents gave better yields because of their participation in hydrogen bonding that forms a powerful intermolecular force with the reactants efficiently. On the other hand aprotic solvents result in lower yields because of lack of O-H and N-H bonds and cannot form hydrogen bond with the reactants. When compared to the yields in different solvents, nickel nano catalyst under solventless condition has been found to give quinoline in a high yields (96 %) (Table 1), the two component cyclization reaction carried out effectively with high selectivity using reflux condition without solvent has been chosen for further study.

The optimization of the reaction conditions and to investigate the behaviour of various 2-amino aryl ketones with acyclic, cyclic ketones and β-keto esters in the presence of catalytic amount of NiNPs was carried over. The compound **3a** was taken as representative example which was synthesized by taking 2-amino benzophenone, **1a** with cyclohexane-1,3-dione, **2** in the presence of catalytic amount of nickel under solventless conditions. In order to evaluate scope and limitation of the reaction, the reaction conditions and the concentration of the nickel nano catalyst was varied and optimized as 10 mol %, where high yields of the product 96 % have been achieved without any by products (Table.2). On further increase in the concentration of the catalyst, the raise in the yields of the product remains unaffected. However in the absence of nickel nano catalyst the reaction did not proceed even for longer reaction time.

The biofabricated nickel nano catalyst under solventless conditions indeed displayed better activity both for cyclic as well as acyclic ketones. The Lewis acid sites present in the nickel nano catalyst effectively interacts with the carbonyl oxygen of ketone through the formation of surface bound hydrogen bonded species which further undergoes Intramolecular cyclization to generate the target molecules in a good yield (Table.3).

2.2 Reusability of the catalyst

The catalyst was filtered off from the reaction mixture at the end of the reaction. It was washed with hot ethanol and water, dried and activated at 250 ˚C for 3 h. The catalyst was reused as such for successive experiments up to five cycles (Fig.3) under similar reaction conditions. It was observed that the morphology of the nickel nano catalyst remains unaffected and moreover there was only a slight difference in the yields of the product thereby showing reusability and recyclability of the nano catalyst without any considerable loss in the catalytic activity. The reusability of the catalyst was examined on the reaction of 2-amino

View Article Online
DOI: 10.1039/C5RA06593C

benzophenone with cyclohexane-1,3-dione to afford quinolines in 96 to 92 %. A comparative study has been carried out on the efficiency of various catalysts reported in literature along with nickel nano catalyst in the synthesis of quinoline derivatives through Friedlander hetero annulation (Table.4).

2.3 UV-Visible spectrum of nickel nano catalyst

The UV-Visible spectrum of nickel nano catalyst in water was recorded against time of reaction by using UV-Visible spectrophotometer. The UV-Visible pattern of nickel nano catalyst before and after the reaction was monitored in the range of 200-800 nm where distinct broad bands were observed at 272 and 274 nm in the ultraviolet region which was very close to the calculated optical spectrum of various metal nanoparticles both in water and in vacuum by Creighton and Eadon based on Mie's theory [69]. The results showed that the stability of the nickel nanocatalyst remains unaffected after five cycles (Fig. 4A, 4B)

2.4 X-ray diffraction pattern of nickel nano catalyst

XRD analysis of recovered nickel nano catalyst showed three intense peaks in the spectrum 2θ scale ranging from 10 to 80. The XRD pattern of recovered nickel nano catalyst agrees well with the standard pure crystalline nickel structures published by the Joint Committee on Powder Diffraction standards (File no: 04-0850) confirmed that the nickel nano catalyst are in crystalline form with face centered cubic (FCC) structure. The presence of nickel nano catalyst results in the formation of Bragg's peaks at 2θ values of 44.18º, 50.92º and 74.16º can be indexed as (111), (220), (200) planes of FCC nickel (Fig.4D). Similarly the presence of nickel nano catalyst (before reaction) results in the formation of Bragg's peaks at 2θ values of 44.39º, 51.26º and 74.68º can be indexed as (111), (220), (200) planes of FCC nickel. (Fig.4C). The results revealed that the morphology of the nickel nano catalyst remains the same after five cycles.

2.5. EDAX pattern of nickel nano catalyst

Energy dispersive X-ray (EDAX) analysis on various regions confirms the presence of nickel nano catalyst with energy bands centered at 7.5 and 8.3 keV [K lines] and 0.8 keV [L lines]. The oxygen and carbon peaks are negligible in EDAX pattern of nickel nano catalyst (before reaction) whereas the oxygen and carbon peaks detected in EDAX pattern of the recovered catalyst was mainly attributed to partial oxidation of the catalyst during handling and due to the interaction with solvent during the workup process (Fig.5A, 5B)

***In-silico* molecular docking studies**

The protein-ligand based interaction plays a significant role in structural based drug design. The most stable docking structure of synthesized quinoline derivatives complexed with histone deacetylase receptor as shown in (Fig .6) clearly indicate that the synthesized ligands are having stronger binding interactions with the receptor which was compared to that of standards Vorinostat and Panobinostat. Ligprep is a versatile conversion program that can be configured to generate ligand libraries with desired structural and chemical features can significantly streamline the entire *in-silico* drug discovery process. It also applies filters to eliminate ligand that does not meet the user specified criteria, allowing the generation of customized library. By using Ligprep accurate, energy minimized 3D molecular structures of poly substituted quinoline [ligand] derivatives were generated. The final 3D quinoline ligands possess various ionization states and ring confirmations with broad chemical and structural diversity. The results (Table.5) obtained from the docking studies have showed that the compounds 7-chloro-3,3-dimethyl-9-phenyl-3,4-dihydroacridin-1(2*H*)-one **3h** (-7.3), 3,3, 9-trimethyl-3,4-dihydroacridin-1(2*H*)-one (-7.1) **3n,** 7-chloro-9-phenyl-2,3-dihydro-1*H*-cyclo penta [b] quinoline **3l** (-6.5), 3,3-di methyl-9-phenyl-3,4-dihydro acridin-1(2*H*)-one **3b** (-6.7), are having better binding affinity showing docking score which is greater than that of standard Vorinostat (-6.4) and comparable to that of the standard Panobinostat (-7.9). The compound 7-chloro-3,3-dimethyl-9-phenyl-3,4-dihydroacrid in-1(2*H*)-one, **3h** posses good lipophilic character mainly because of the presence of halogen and two methyl groups as substituents. Ligand binding induces confirmational changes in the protein, such as loop motions or domain reorientations. The affinity and specificity of the binding interactions of the ligands were mainly determined by the structural and physicochemical properties of the binding partners. Moreover there is no significant change has been observed in the final geometry of the synthesized ligands after interaction with the receptor.

Increase in lipophilic nature makes the molecule more polarized and accordingly the London dispersion force increases which are quite necessary for the lipophilic substances to interact within themselves and other amino acid residues in the receptor. From the results it can be understood that the compounds **3h**, **3n**, **3l**, **3b** possess good anticancer efficacy as histone deacetylase inhibitors (HDIs). Histone deacetylase inhibitors are cytostatic agents that inhibit the proliferation of cells and arrest cell cycle there by inducing apoptosis. In order to carry out gene expression normally, the coiling and uncoiling of DNA around histones should be primarily controlled. This process is accomplished with the support of histone acetyl transferases (HAT), where the lysine residues in core histones are acetylated with the formation of less compact, transcriptionally active chromatin where as histone deacetylases (HDAC) leads to the formation of condensed and transcriptionally silenced chromatin by effectively removing the acetyl groups from the lysine residues. This reversible mechanism is very vital for controlling and regulating the gene expression and in remodelling the topology of chromatin structure. The synthesized quinoline derivatives selectively block the deacetylation of lysine residues which subsequently causes hyperacetylation of histones with altered gene expression (Fig.7).

3 Experimental

3.1 Materials and methods

Solvents and reagents were commercially sourced and used without further purification. Thin layered chromatography (TLC) was performed on preparative plates of silica gel and visualization was made with iodine chamber. Column chromatography was performed by using silica gel (100-200 mesh). Melting points were measured on Elchem Microprocessor based DT apparatus using an open capillary tube and are corrected with standard benzoic acid. The NMR spectra were recorded on a Bruker Avance III – 400 MHz spectrometer using TMS as internal standard (chemical shifts δ in ppm). GC-MS was recorded on Perkin Elmer: clarus 680/600.

3.1.1 Biofabrication of nickel nano catalyst

The biosynthesis of nickel nano catalyst from *Aegle Mearmelos* Correa aqueous leaf extract was reported in our previous work [70].

View Article Online
DOI: 10.1039/C5RA06593C

3.1.2 Characterization of nickel nano catalyst

The surface morphology of the synthesized nickel nano catalyst was studied by using SEM analysis. The results obtained from SEM showed that the nanoparticles are crystalline in nature with traingle shape having an average particle size of 80-100 nm. (Fig.8A, 8B)

The metal nanoparticles are generally unstable, and exploration of their stability is a key factor in their successful and wide applications in heterogenous catalysis. In order to observe the characteristic weight loss of biosynthesized NiNPs with rise in temperature thermogravimetric analysis were carried out by using Shimadzu DT-50 thermal analyser at a heating rate of 10 °C/min was applied to NiNPs. The thermal analysis curve of the Nickel NPs showed a steady weight loss in the temperature of 100-800 °C (Fig.8C).

3.1.3 Synthesis of quinoline derivatives

The synthetic strategy leading to the key precursors and target compounds was illustrated in (Scheme.1). The compounds were prepared by the reaction of 2-aminoaryl ketone with enolisable ketone in the presence of NiNPs as a catalyst under solvent-free conditions.

3.1.4 General procedure for the synthesis of quinoline derivatives

In a round bottom flask 2-aminoaryl ketone (1 mmol) and enolisable ketone (1 mmol) and catalytic amount of NiNPs was added under stirring at room temperature for 10 min. Later the reaction was carried out in an oil bath at 75 ˚C. The progress of the reaction was monitored under TLC and after completion the reaction mass was cooled to room temperature and extracted by using ethylacetate as solvent. The catalyst was seperated from the crude reaction mixture by normal filtration. The organic layer containing crude reaction mass was separated and dried over anhydrous sodium sulphate, then concentrated under reduced pressure. Further purification of the reaction was done by column chromatography in 100-200 mesh silica gel using petroleum ether :ethyl acetate (10 : 1 v/v) as the eluting solvent system. Further characterization of the products was carried by spectral analysis using FT-IR, ^{1}H NMR, ^{13}C NMR and GC-MS.

3.1.5 In-silico molecular docking studies

The docking analysis of final quinoline derivatives **3a-s**, reference ligand and standards Vorinostat, Panobinostat was carried out using Schrodinger molecular docking software. The X-ray crystal structure of histone deacetylase receptor (ID-1ZZ3) was taken from protein data bank[77]. The active site of histone deacetylase receptor was well established with hydrophobic active site containing irreversible inhibitor. In order to distinguish the basic ligand-receptor interactions molecular docking simulations were carried out and protein was prepared by protein preparation wizard where it is preprocessed by simultaneously deleting the substrate cofactors as well as crystallographically depicted water molecules and optimizing hydrogen bonds. Finally after assigning charge and protonation state energy minimization with root mean square deviation (RMSD) of 0.35 A˚ was done using OPLS2005 force field. Receptor grid was prepared with default parameters without having any constraints and sites were created around the reference ligand (3-Cyclopentyl-*N*-Hydroxypropanamide) of histone deacetylase. The structures of the ligands were drawn using Maestro 8.5. The ligands were prepared using Ligprep utility of Schrodinger software where hydrogen atoms addition option was enabled, unwanted molecules such as water and small ions are filtered out based on the properties of the ligands. Charge groups are neutralized and ionization states were created by using Epik option. Finally the geometries of the ligands were optimized by generating low energy ring confirmations. The ligands did not show any signs for the formation of isomers or tautomers after Ligprep. The ligands docking were carried out with Xtra precision mode (XP) option employed in Glide (5.5) module implemented in Shrodinger LLC. In the present version both the receptor as well as ligand kept fixed and for each derivative various confirmations have been screened at different poses within the receptor. Finally the most stable confirmations were selected and subjected to glide virtual simulation with optimization option using Tripos force field and applying Gasteiger-Huckel charges. The rototranstional area in to which the ligand is allowed to move freely around the active sphere is restricted to 10 A˚. The derivatives of the final compounds were docked with the receptor and the interactions of ligands with the receptor were shown.

Conclusions

A cost-effective, ecofriendly protocol has been developed for the synthesis of polysubstituted quinoline derivatives through Friedlander annulation. This one pot nickel nano catalysed synthesis of quinoline derivatives is unique alternative route for rapid generation of structurally diversified quinoline derivatives with high yields under solvent free conditions with shorter reaction time. The remarkable reusability, selectivity and environmental compatibility are among the other added advantages to make this approach an efficient route for the production of the target molecules. From the *in-silico* molecular docking studies it can be concluded that the synthesized quinolines possess excellent anticancer properties as histone deacetylase inhibitors and in future research has to be carried out in exploring the anticancer properties of the quinoline derivatives in *in-vivo* models.

Ackowledgements

The authors sincerely thank the management of VIT University, Vellore, Tamil Nadu, India for their constant encouragement and support and providing all the necessary facilities for carrying out this study. The authors also thank DST-VIT-FIST, SIF-VIT for carrying out NMR analysis.

Notes and references

[a] *Organic Chemistry Division, School of Advanced Sciences, VIT University, Vellore 632014, Tamilnadu, India. Fax: 91-416 224 3092; Tel: 0416 220 2352; E-mail: dr.subashini.r@gmail.com;.*

1. R.D. Larsen, E.G. Corley, A.O. King, J.D. Carrol, P. Davis, T.R. Verhoeven, P.J. Reider, M. Labelle, J.Y. Gauthier, Y.B. Xiang and R.J. Zamboni, *J. Org. Chem.*,1996, **61**, 3398–3405.
2. Y.L. Chen, K.C.Fang, J.Y. Sheu, S.L.Hsu and C.C.Tzeng, *J. Med. Chem.*, 2001, **44**, 2374–2377.
3. G. Roma, M.D. Braccio, G. Grossi, F. Mattioli and M. Ghia, *Eur. J Med. Chem.*, 2000, **35**:1021–1035
4. P.M.S. Chauhan and S.K. Srivastava, *Curr. Med. Chem.*, 2001, **8**, 1535-1542.

View Article Online
DOI: 10.1039/C5RA06593C

5. P.M. Dewick, Medicinal natural products: a biosynthetic approach. John Wiley and Sons, 2009, third edition.
6. W. Peters and W.H.G. Richards. Antimalarial Drugs II; Eds.; Springer Verlag: Berlin Heidelberg, New York, Tokyo. *Phys*.,1984, **8**, 311-314.
7. K.H. Chikhalia, M.J. Patel and D.B. Vashi, *Arkivoc*., 2008, **xiii**, 189-197.
8. V.Kumar, A.Mahajan and K.Chibale, *Bioorg. Med. Chem*., 2009,**17**, 5433-5441.
9. M.Sachin, A.Choudhary, S.Kumar and G. Avasthi, *Journal of Pharmacy Research*., 2010, **3**, 1519-1523.
10. J.K.Stille, *Macromolecules*.,1981, **14**, 870–880
11. A.K.Agrawal and S.A. Jenekhe, *Macromolecules*., 1991, **24**, 6806–6808
12. A.K. Agrawal and S.A. Jenekhe, *Chem Mater*., 1993, **5**,633–640
13. G. Jegou and S.A. *Macromolecules*., 2001, **34**,7926–7928
14. X. Zhang, A.S. Shetty and S.A. Jenekhe, *Macromolecules*., 2000, **33**, 2069–2082
15. M.I. Anderson and A.P. MacGowan, *J. Antimicrob. Chemoth*., 2003, **51**, 1-11.
16. H.I. Abd-Alla, M. Shaaban, K.A. Shaaban, N.S. Abu-Gabal, N.M. Shalaby and H. Laatsch, *Nat. Pro. Res*., 2009, **23**, 1035-1049.
17. K. Goto, K.Yabe, T. Suzuki, T. Jindo and A. Sanbuissho, *Toxicology*., 2010, **276**,122-127.
18. P.M. Hawkey, *J. Antimicrob. Chemoth*., 2003, **51**, 29-35.
19. M. Malik, G. Hoatam, K. Chavda, R.J.Kerns and K. Drlica, *Antimicrob. Agents Chemother*., 2010, **54**, 149-156.
20. J. Minville, J. Poulin, C. Dufresne and C.F. Sturino, *Tetrahedron Lett*., 2008, **49**, 3677-3681.
21. X. Guo, YL. Li, YF. Liu, H.Y.Gou and Y.C.Wang, *Chin. Chem. Lett*., 2010., **21**, 1141-1144.
22. M.F. Grundon, *Nat. Pro. Rep*., 1990, **7**, 131-138.
23. J.P. Michael, *Nat. Prod. Rep*., 2007, **25**, 166-187.
24. Y. Chen, Y.Zhao, C. Lu, C. Tzeng and J.P. Wang, *Bioorg. Med. Chem*., 2006, **14**, 4373–4378.
25. J.P. Sanchez, J.M. Domagala, S.E. Hagen, C.L.Heifetz, M.P.Hutt, J.B.Nichols and A.K. Trehan, *J. Med. Chem*., 1988, **31**, 983–991.
26. K. Raynes, M. Foley, L. Tilley and L.W. Deady, *Biochem. Pharmacol*., 1996, **52**, 551–559.
27. A.R. Gholap, K.S. Toti, F. Shirazi, R.Kumari, M.K. Bhat, M.V. Deshpande and K.V. Srinivasan, *Bioorg. Med. Chem*., 2007, **15**, 6705–6715.
28. A. Fournet, A.A. Barrios, V.Munoz, R. Hocquemiller, A.Cave and J. Bruneton, *Antimicrob. Agents Chemother*., 1993, **37**,859–863.
29. A.H. Abadi, G.H. Hegazy and A.A.E. Zaher, *Bioorg. Med. Chem*., 2005, **13**, 5759–5765.
30. J. Ghosh, V. Swarup, A. Saxena, S.Das, A. Hazra, P. Paira, S. Banerjee, N.B. Mondal and A. Basu, *Int. J. Antimicrob. Agents*., 2008, **32**, 349–354.
31. D.A.Scott, C.L. Balliet, D.J. Cook, A.M.Davies, T.W. Gero, C.A. Omer, S. Poondru, M.E. Theoclitou, B. Tyurin and M.J. Zinda, *Bioorg. Med. Chem. Lett*., 2009, **19**, 697–700.
32. R.C. Bernotas, R.R. Singhaus, D.H. Kaufman, J. Ullrich, H. Fletcher, E. Quinet, P. Nambi, R.Unwalla, A. Wilhelmsson, A.G.Nilsson, M. Farnegardh and J.Wrobel, *Bioorg. Med. Chem*., 2009, **17**, 1663–1670.
33. V.V. Kouznetsov, L.Y.V. Mendez and C.M.M. Gomez, *Curr. Org. Chem*., 2005, **9**, 141-161.
34. F. Xiao, Y. Chen, Y. Liu and J. Wang, *Tetrahedron*., 2008, **64**, 2755-2761.
35. M.Z. Hoemann, G. Kumaravel, R.L. Xie, R.F. Rossi, S .Meyer, A. Sidhu, G.D. Cuny and J.R. Hauske, *Bioorg. Med. Chem. Lett*., 2000, **10**, 2675-2678.
36. P.G.Dormer, K.K. Eng, R.N.Farr, G.R.Humphrey, J.C. McWilliams, P.J. Reider, J.W.Sager, and R.P. Volante, *J. Org. Chem*., 2003, **68**, 467–477.
37. M. Matsugi, F.Tabusa and J. Minamikawa, *Tetrahedron Lett*., 2000, **41**, 8523–8525.
38. R.H. Mansake and M. Kulka, *Org React*., 1953, **7**, 59–98.
39. M.E. Theoclitou and L.A. Robinson, *Tetrahedron Lett*., 2002, **43**, 3907–3910.
40. Y.L. Chen, K.C.Fang, J.Y. Sheu, S.L.Hsu and C.C.Tzeng, *J.Med. Chem*., 2001, **44**, 2374–2377.
41. R.D. Larsen, E.G. Corley, A.O. King, J.D. Carrol, P. Davis, T.R. Verhoeven, P.J. Reider, M. Labelle, J.Y. Gauthier, Y.B. Xiang and R.J. Zamboni, *J. Org. Chem*.,1996, **61**, 3398–3405.
42. A. Arcadi, M. Chiarini, S.D. Giuseppe and F. Marinelli, *Synlett*., 2003, **2**, 0203–0206.
43. E.A. Fehnel. *J. Org. Chem*., 1966, **31**, 2899–2902.
44. P. Arumugam, G. Karthikeyan, R. Atchudan, D. Muralidharan and P.T. Perumal, *Chem Lett*., 2005, **34**, 314–315.
45. J.Wu, L. Zhang and T.N. Diao, *Synlett*., 2005, **17**, 2653–2657
46. B.R. McNaughton and B.L. Miller, *Org Lett.,* 2003, **5**, 4257–4259
47. J.S. Yadav, P.P. Rao, D. Sreenu, R.S. Rao, V.N. Kumar, K. Nagaiah and A.R. Prasad, *Tetrahedron Lett*., 2005, **46**, 7249–7253
48. J.S. Yadav, B.V.S Reddy, P. Sreedhar, R.S. Rao and K. Nagarah, *Synthesis*., 2004, **14**, 2381–2385.
49. M.A. Zolfogol, P. Salehi, A. Ghaderi, M. Shiri and Z. Tanbakouchian, *J Mol Cat A Chem*., 2006, **259**, 253–258.
50. P.Bandyopadhyay, G.K. Prasad, M. Sathe, P.Sharma, A.Kumar and M.P.Kaushik, *RSC Adv*., 2014, **4**, 6638-6645.
51. B. Palakshi Reddy, P. Iniyavan, S. Sarveswari and V. Vijayakumar, *Chin. Chem. Lett*., 2014, **25**, 1595-1600.
52. A. Corma and H.Garcia, *Catal.Today*. 1997, **38**, 257-308.
53. S.K. Sikdar and S.G.J.Howell, *Cleaner Production*., 1998, **6**, 253-259.
54. G.M. Whitesides, *Nat. Biotechnol*., 2003, **21**, 1161-1165.
55. R. Narayanan and M.A. El-Sayed, *J. Am. Chem. Soc*., 2004, **126**, 7194–7195.
56. K.D. Bhatte, K.M. Deshmukh, Y.P. Patil, D.N. Sawant, S.I. Fujita, M. Arai and B.M. Bhanage, *Particuology*., 2012, **10**, 140-143.
57. I. Ban, J.Sterger, M. Drofenic, G. Ferk and D. Makovec, *J. Magn. Magn. Mater.*, 2011, **323**, 2254-2258.
58. M.Kidwai, V.Bansal, A.Saxena, R.Shankar and S.Mozumdar, *Tetrahedron*., 2006, **47**, 4161-4165.
59. F.Aonso, P.Riente and M. Yus, *Tetrahedron*., 2008, **64**, 1847-1852.
60. A.Saxena, A.Kumar and S.Mozumdar, *J. Mol. Catal. A: Chem*., 2007, **269**, 35-40.
61. Y.Tang, D. Yang, F.Qin, J.Hu, C.Wang and H.Xu, *J. Solid State Chem*., 2009, **182**, 2279-2284.
62. I.Vicente, P.Salagre and Y.Cesteros, *Appl. Clay. Sci*., 2011, **53**, 212-219.
63. A.Saxena, A.Kumar and S.Mozumdar, *Appl. Catal. A : Gen*., 2007, **317**, 210-215.
64. A. Kumar, S. Kumar, A. Saxena, A. De and S. Mozumdar, *Catal. Commun*., 2008, **9**, 778-784.
65. A.Bell, The Impact of Nanoscience on Heterogeneous Catalysis. *Science*., 2003, **299**, 1688–1691.
66. G.W. Wang and C.S. Jia, *Lett. Org. Chem*., 2006, **3**, 289–291.
67. M.Hosseini-Sarvari, *J. Iran. Chem. Soc*., 2011, **8**, S119-S128.
68. G. Salvatore, E. Francesco, M. M. Carla, P. Caroline and C. Massimo, *Tetrahedron Lett*., 2011, **52**, 3474-3477.
69. S. Ebrahim, K. M. Mehdi, B. Nasim and S. Saadi, *Chem. Pharm. Bull*., 2010, **58**, 212-213.
70. H. Fang, Z. Ji-ming, Y. Zhi-jun and Z. Jian-hua, *Shandong Kexue*., 2010, **23**, 6-10.
71. S. K. De and R.A. Gibbs, *Tetrahedron Lett*., 2005, **46**, 1647-1649.
72. J.S. Yadav, B.V.S. Reddy, V. Sunitha, K. Srinivasa Reddy and K.V.S. Ramakrishna, *Tetrahedron Lett*., 2004, **45**, 7947–7950.
73. J. Mohammad nezhad, J. Akbari, A. Heydari and B. Alirezapour, *Bull. Korean. Chem. Soc*., 2011, **32**, 3853-3854.
74. H.S. Mona, *Can. J. Chem.*, 2009, **87**, 1122-1126.
75. J.A. Creighton and D.G. Eadon, *J. Chem. Soc*., 1991, **87**, 3881-3891.
76. G. Angajala, R. Ramya and R. Subashini, *Acta Trop*., 2014, **40,** 19-26.
77. T.K. Nielsen, C. Hildmann, A. Dickmanns, A. Schwienhorst, .Ficner, *J.Mol.Biol*., 2005, **354**, 107-120.

View Article Online
DOI: 10.1039/C5RA06593C

View Article Online
DOI: 10.1039/C5RA06593C

FIGURE CAPTIONS

Fig.1 Plausible reaction mechanism for the synthesis of polysubstituted quinolines using nickel nanoparticles.

Fig.2 FT-IR spectrum of nickel nanoparticles (80-100 nm).

Fig.3 Reusability of the nickel nano catalyst (80-100 nm) for the synthesis of 9-phenyl-3, 4-dihydroacridin-1(2H)-one (**3a**).

Fig.4 [A] UV-Visible analysis of nickel nano catalyst (before reaction) [B] UV-Visible analysis of nickel nano catalyst [after recovery] [C] XRD analysis of nickel nano catalyst (before reaction) [D] XRD analysis of nickel nano catalyst (after recovery).

Fig.5 [A] EDAX pattern for nickel nano catalyst (before reaction) [B] EDAX pattern for nickel nano catalyst (after recovery).

Fig.6 *In silico* molecular docking studies of quinoline derivatives as histone deacetylase inhibitors (HDIs). [A] The binding interaction of 7-chloro-3, 3-dimethyl-9-phenyl-3, 4-dihydroacridin-1(2*H*)-one **3h** with histone deacetylase receptor. [B] The binding interaction of 3, 3, 9-trimethyl-3, 4-dihydroacridin-1(2*H*)-one **3n** with histone deacetylase receptor. [C] The binding interaction of 7-chloro-9-phenyl-2, 3-dihydro-1*H*-cyclopenta[b]quinoline **3l** with histone deacetylase receptor. [D] The binding interaction of 3, 3-dimethyl-9-phenyl-3, 4-dihydro acridin-1(2*H*)-one **3b** with histone deacetylase receptor.

Fig.7 Mechanism of action for anticancer efficacy of synthesized quinoline derivatives.

Fig.8 [A] SEM pattern for nickel nano catalyst (Magnification at 13700x) [B] SEM pattern for nickel nano catalyst (Magnification at 24600x) [C] Thermogravimetric analysis of nickel nano catalyst.

Scheme.1 Synthesis of polysubstituted quinolines using nickel nanoparticles.

View Article Online
DOI: 10.1039/C5RA06593C

List of tables

Table.1 Effect of solvent in the synthesis of 9-phenyl-3, 4-dihydroacridin-1(2H)-one (**3a**) [a]

Entry	Solvent	Catalyst (mol %)	Yield (%) [b]
1	Acetonitrile	10	55
2	Tetrahydrofuran	10	62
3	Acetone	10	76
4	Acetic acid	10	84
5	Ethanol	10	92
6	Solventless	10	96

[a] Reaction conditions : 2-amino benzophenone, **1a** (1 mmol), Cyclohexane1,3-dione (1 mmol), NiNPs (80-100 nm), 75 ºC.
[b] Isolated yield.

Table.2 Effect of catalyst concentration in the synthesis of 9-phenyl-3, 4-dihydroacridin-1(2H)-one (**3a**) [a]

Entry	Catalyst (mol %)	Time (min)	Yield (%) [b]
1	2.5	220	53
2	5.0	220	65
3	7.5	140	81
4	10.0	50	96
5	12.5	50	96
6	15.0	50	96

[a] Reaction conditions : 2-amino benzophenone, **1a** (1 mmol), Cyclohexane1,3-dione (1 mmol), NiNPs (80-100 nm) Solventless, 75 ºC.
[b] Isolated yield.

View Article Online
DOI: 10.1039/C5RA06593C

Table.3 Synthesis of quinolines and polysubstituted quinolines using NiNPs [a] (80-100 nm)

Entry	Amino Ketone	Enolisable Ketone	Product	Time (min)	Yield (%) [b]
1	1a		3a	50	96
2	1a		3b	50	95
3	1a		3c	55	92
4	1a		3d	65	94
5	1a		3e	68	89
6	1a		3f	52	95
7	1b		3g	59	92
8	1b		3h	50	94
9	1b		3i	76	96
10	1b		3j	61	92
11	1b		3k	57	89

View Article Online
DOI: 10.1039/C5RA06593C

Table.3 (Continued)

Entry	Amino Ketone	Enolisable Ketone	Product	Time (min)	Yield (%)[b]
12	1b		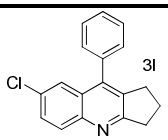 3l	60	95
13	1c	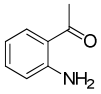	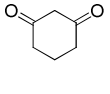 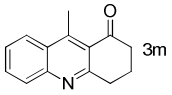 3m	50	92
14	1c	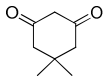	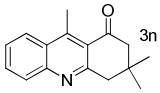 3n	50	95
15	1c	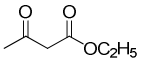	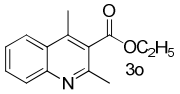 3o	56	90
16	1c	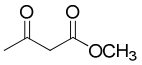	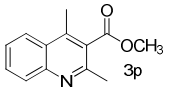 3p	72	94
17	1c	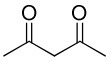	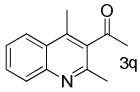 3q	50	92
18	1d	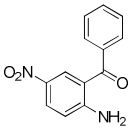	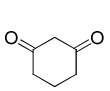 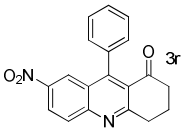 3r	60	87
19	1d	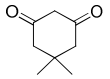	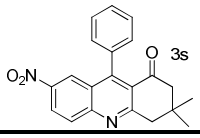 3s	50	93

[a] Reaction conditions : Amino ketone (1 mmol) Ketone (1 mmol) and NiNPs (10 mol %), Solventless, 75 ºC.
[b] Isolated yield.

Table.4 Comparison of efficiency of various catalysts in the Friedlander annulation of quinoline synthesis.

Entry	Catalyst	Time (min)	Yield (%)
1	KSF clay	360	75[66]
1	ZnO NPs	180	75[67]
2	Yb[OTf]$_3$	60	75[68]
2	Cu(CF$_3$SO$_3$)$_2$	300	80[69]
3	SbCl$_3$	300	82[70]
4	Y(OTf)$_3$	240	83[71]
5	Bi (OTf)$_3$	180	86[72]
5	CuO NPs	300	88[73]
6	ZrO$_2$	210	92[74]
7	NiNPs	50	96

View Article Online
DOI: 10.1039/C5RA06593C

Table.5 *In silico* molecular docking results of synthesized quinoline derivatives, reference ligand and standards.

Entry	Ligand	Glide Score [XP]	Lipophilicity	Hydrophobicity
1	3a	-4.5	-2.5	-0.5
2	3b	-6.7	-3.9	-1.4
3	3c	-5.3	-3.2	-0.8
4	3d	-4.8	-2.3	-0.5
5	3e	-5.6	-3.4	-1.1
6	3f	-4.0	-2.4	-0.9
7	3g	-6.3	-4.0	-0.7
8	3h	-7.3	-4.3	-0.4
9	3i	-6.2	-3.6	-1.2
10	3j	-5.9	-3.4	-0.5
11	3k	-5.6	-3.1	-1.0
12	3l	-6.5	-3.8	-0.4
13	3m	-6.0	-3.5	-0.8
14	3n	-7.1	-3.3	-1.5
15	3o	-4.8	-2.7	-1.1
16	3p	-5.3	-3.0	-0.5
17	3q	-5.9	-3.2	-0.2
18	3r	-5.4	-2.1	-0.9
19	3s	-5.8	-3.2	-0.4
20	Reference Ligand[a]	-8.5	-4.8	-1.2
21	Std[b]	-6.4	-3.9	-0.3
22	Std[c]	-7.9	-4.5	-0.5

[a] 3-Cyclopentyl-N-Hydroxypropanamide; [b] Vorinostat; [c] Panobinostat.

View Article Online
DOI: 10.1039/C5RA06593C

Fig.1

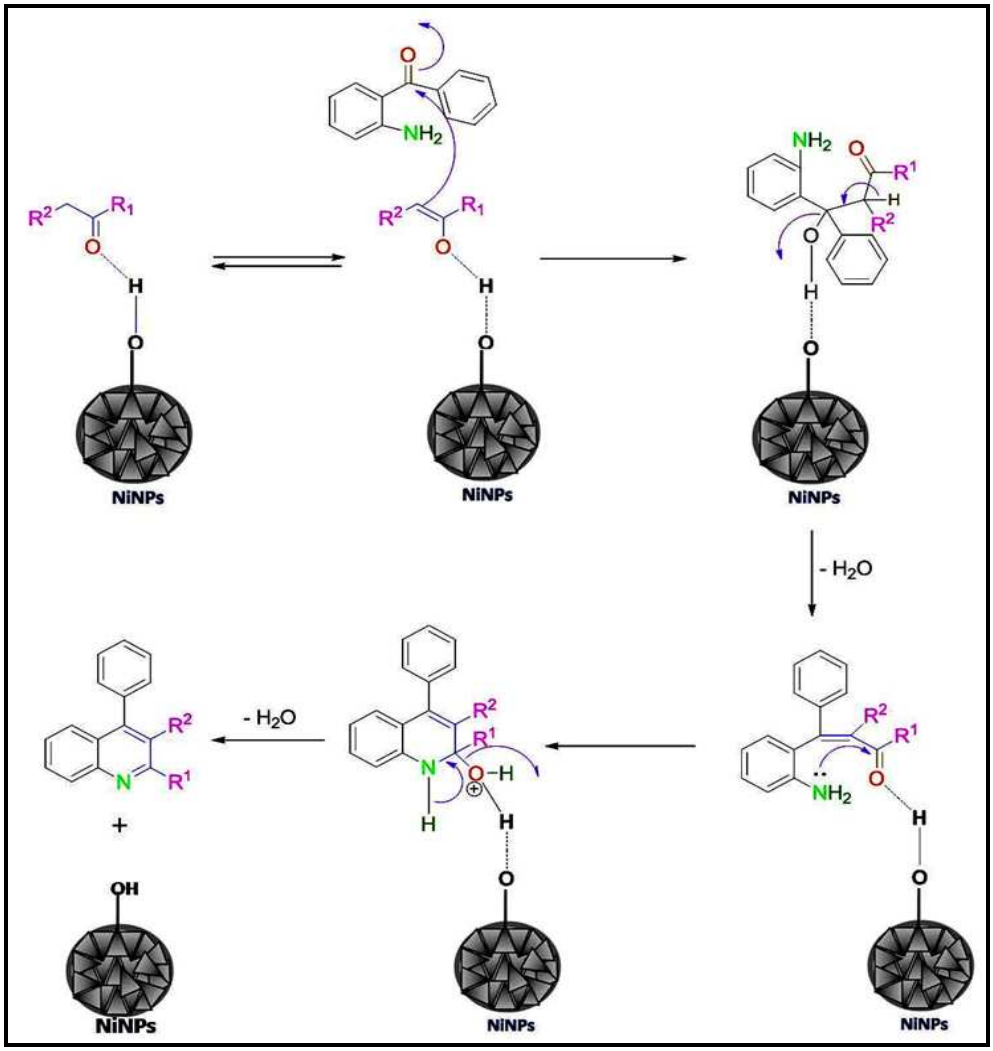

View Article Online
DOI: 10.1039/C5RA06593C

Fig.2

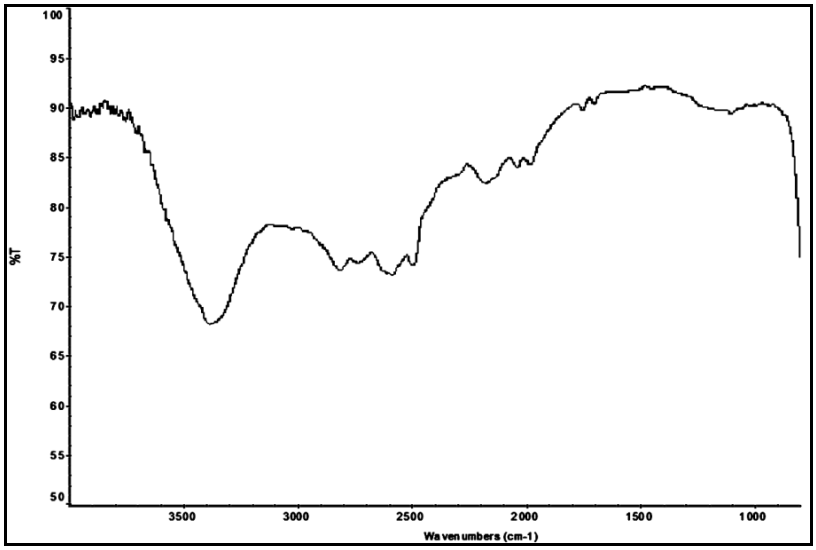

View Article Online
DOI: 10.1039/C5RA06593C

Fig.3

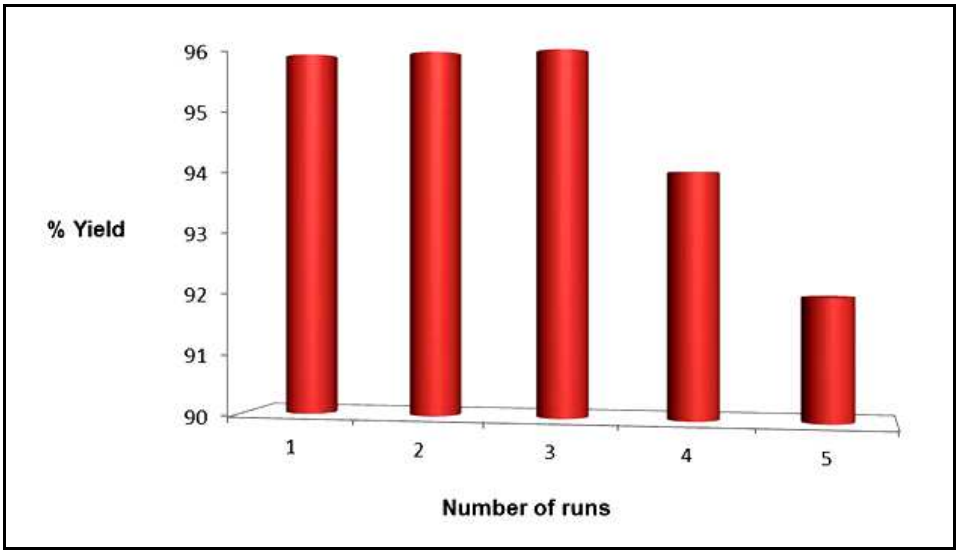

View Article Online
DOI: 10.1039/C5RA06593C

Fig.4

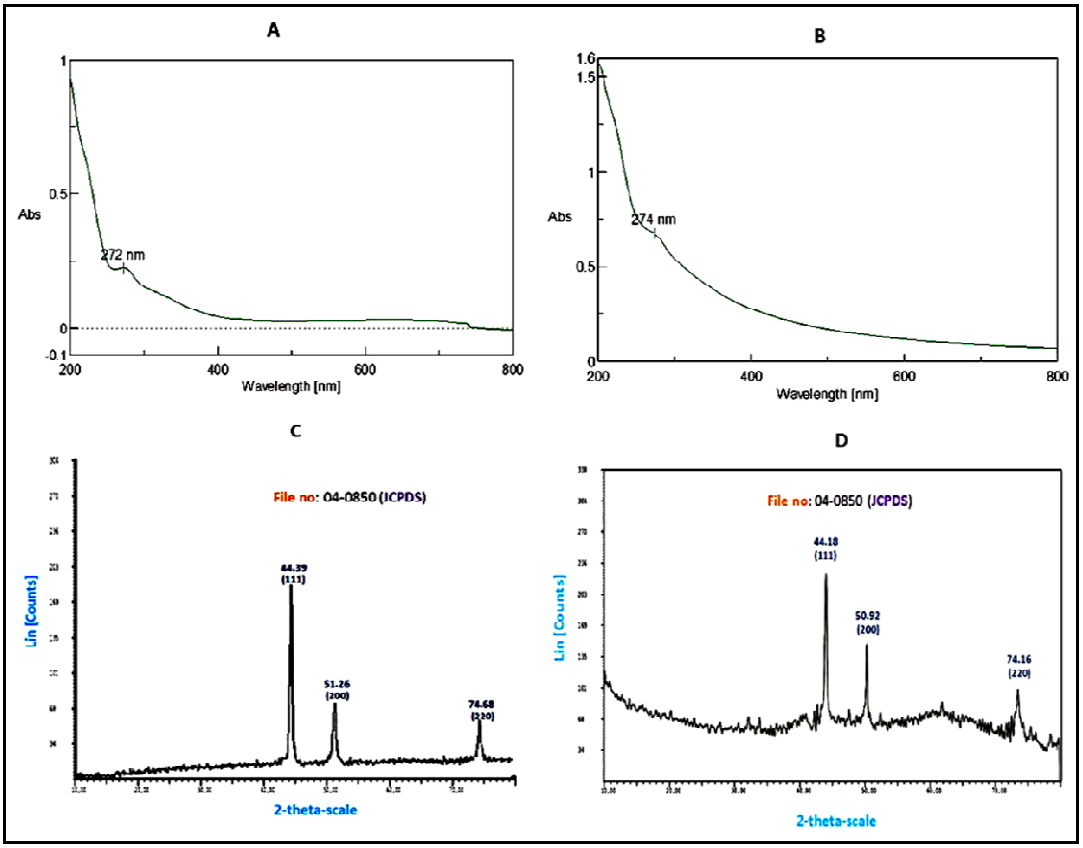

View Article Online
DOI: 10.1039/C5RA06593C

Fig.5

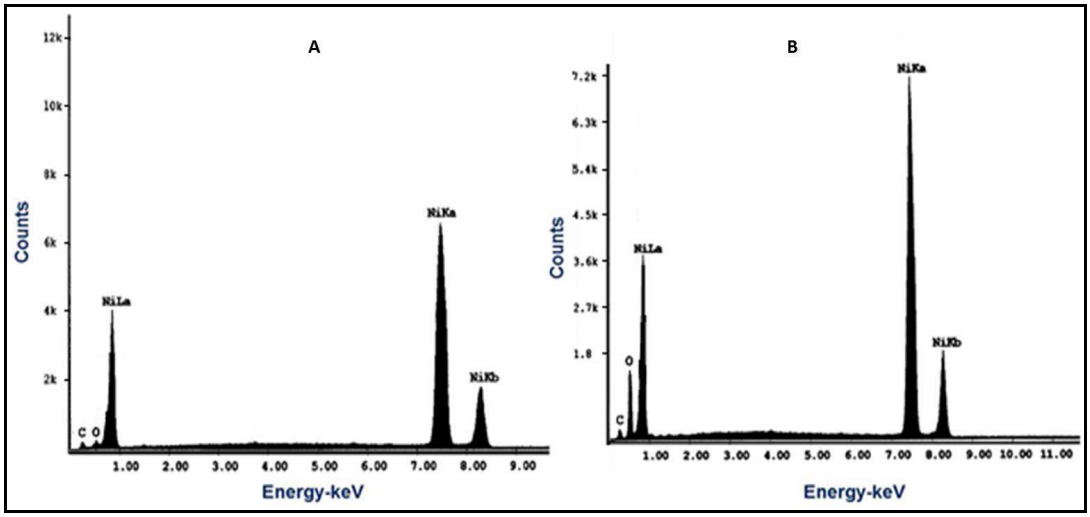

View Article Online
DOI: 10.1039/C5RA06593C

Fig.6

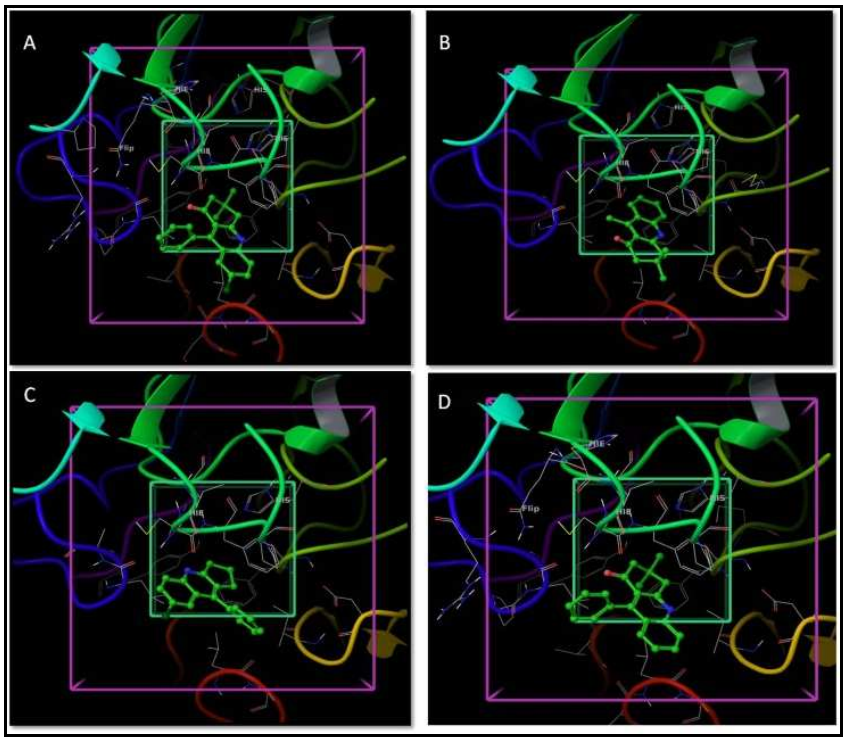

View Article Online
DOI: 10.1039/C5RA06593C

Fig. 7

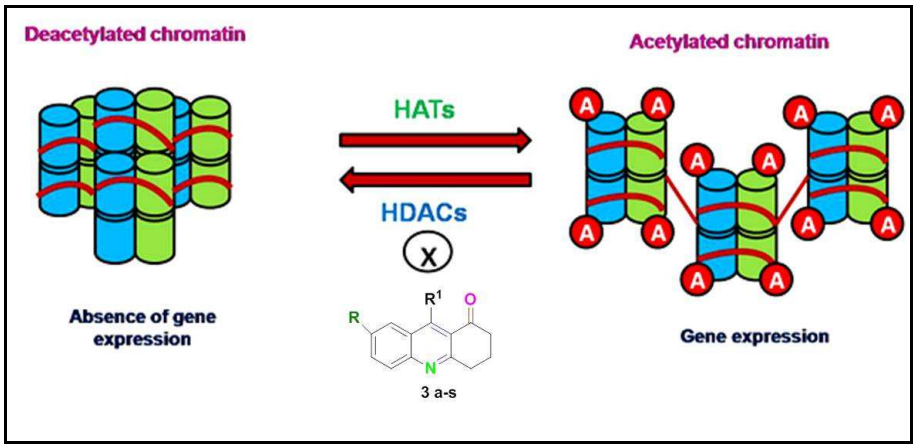

View Article Online
DOI: 10.1039/C5RA06593C

Fig. 8

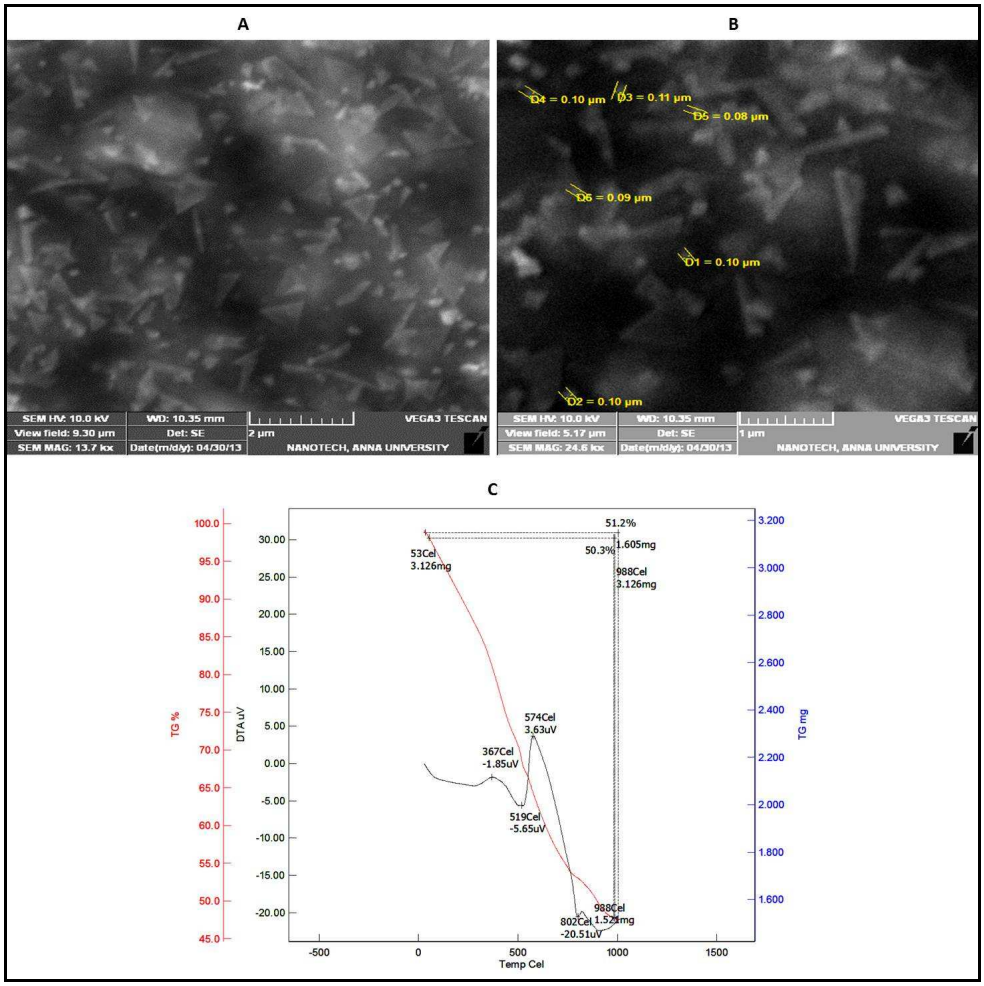

View Article Online
DOI: 10.1039/C5RA06593C

Scheme.1